European Journal of Mechanics A/Solids 45 (2014) 226–237

Contents lists available at ScienceDirect

European Journal of Mechanics A/Solids

journal homepage: www.elsevier.com/locate/ejmsol

Parameter identification of a thermodynamic model for superelastic shape memory alloys using analytical calculation of the sensitivity matrix

F. Meraghni [a], Y. Chemisky [a,*], B. Piotrowski [a], R. Echchorfi [a], N. Bourgeois [b], E. Patoor [a]

[a] Arts et Métiers ParisTech, LEM3-UMR 7239 CNRS, 4 Rue Augustin Fresnel, 57078 Metz, France
[b] Université de Lorraine, LEM3-UMR 7239 CNRS, Ile du Saulcy, 57045 Metz, France

ARTICLE INFO

Article history:
Received 4 December 2012
Accepted 24 December 2013
Available online 7 January 2014

Keywords:
Analytical sensitivity calculation
Shape memory alloys
Thermodynamical constitutive modeling

ABSTRACT

This paper presents an identification procedure for the parameters of a thermodynamically based constitutive model for Shape memory Alloys (SMAs). The proposed approach is a gradient-based method and utilizes an analytical computation of the sensitivity matrix. For several loading cases, including superelasticity, that are commonly utilized for the model parameters identification of such a constitutive model, a closed-form of the total infinitesimal strain is derived. The partial derivatives of this state variable are developed to find the components of the sensitivity matrix. A Levenberg–Marquardt algorithm is utilized to solve the inverse problem and find the best set of model parameters for specific SMA materials. Moreover, a pre-identification method, based on the second derivative of the total strain components is proposed. This provides a suitable initial set of model parameters, which increases the efficiency of the inverse method. The proposed approach is applied for the simultaneous identification of the non-linear constitutive parameters for two superelastic SMAs. The comparison between experimental and numerical curves obtained for different temperatures shows the capabilities of the developed identification approach. The robustness and the efficiency of the developed approach are then experimentally validated.

1. Introduction

Shape memory Alloys are now utilized in a wide range of applications, especially in aerospace, biomedical and energy industrial fields (Otsuka and Wayman, 1999). This success is attributed to their ability to recover substantial deformation when subjected to particular thermomechanical input. Among the number of thermomechanical loading paths that can lead to the appearance of these important deformations, two remarkable paths are often utilized in industrial applications. The first one is an isothermal path at sufficiently high temperature, which induces a superelastic behavior, where significant strains are developed and recovered upon an isothermal mechanical cycling loading. The second typical loading path is an isobaric cooling–heating cycle, where seemingly permanent strains appear during cooling under stress and are recovered upon heating (Lagoudas, 2008). When the temperature is controlled, an SMA component can be actuated, for example to modify the geometry of a structure for morphing applications (Hartl et al., 2010a, 2010b). These two effects are obtained for a specific loading path, but the thermomechanical behavior of SMA is more general and a wide variety of effects can be obtained for different loading paths. This has motivated the development of constitutive models based on the expression of a thermodynamic potential, which allows the description of the material state for all different kinds of loadings. A review of these models for SMAs can be found in Patoor et al. (2006) for the behavior of the single crystal and Lagoudas et al. (2006) for the constitutive modeling of polycrystals.

The design of SMA structures and the optimization of their characteristics are conducted now with the use of numerical simulations, most of them based on finite element analysis (FEA). Most of the three-dimensional constitutive models for SMAs are nowadays implemented in FEA codes. The accuracy of a numerical simulation of the SMA structural behavior relies on the model ability to accurately predict the constitutive behavior but also on the correct estimation of the model parameters, characteristic of a specific alloy. The common way to determine the material parameters related to the phase transformation is defined in two ASTM Standards (F2004, 2005, 2010, F2082, 2006). This methodology, useful to characterize the quality and to get specification acceptance

* Corresponding author. Tel.: +33 387 375 452.
E-mail address: yves.chemisky@ensam.eu (Y. Chemisky).

0997-7538/$ – see front matter © 2014 Elsevier Masson SAS. All rights reserved.
http://dx.doi.org/10.1016/j.euromechsol.2013.12.010

for Nickel–Titanium in the biomedical industry, is not suitable for the identification of a model that aims at performing the numerical simulation of SMA structures. Indeed, the methodology is restricted to the determination of the transformation temperatures. Moreover, this determination may differ according to the method utilized (F2082, 2006).

The development of a reliable method to identify the parameters for SMA constitutive models is thus an important step to be able to perform reliable numerical simulations for the design of SMA structures, regardless of the choice of a constitutive model. The methodology applied to identify the parameters of the constitutive models based on the thermodynamics of the phase transformation often requires the construction of the phase diagram (Lagoudas, 2008; Hartl et al., 2010a, 2010b; Chemisky et al., 2011), instead of following the ASTM standards that does not give indication on the characterization of the complete set of parameters for these models. Several material parameters are obtained based on this phase diagram, which are now well utilized in the SMA community. The most common procedure is a manual procedure where the transformation points are obtained using a tangent intersection method (Stebner et al., 2011). However, several issues are associated to this methodology, since no objective criterions are utilized to assess the efficiency of the method. This can lead to potential error when estimating the model parameters of a SMA material. In this work, an identification approach is proposed to obtain the suitable model parameters that will be utilized for the simulation of the shape memory alloys thermomechanical behavior. This method is focused on the identification of the material parameters to simulate the superelastic response of SMA structures. This kind of behavior is indeed widely utilized in industrial applications (e.g. dentistry, surgical instruments, stents and micro-actuators).

Several strategies have been developed to extract directly the parameters of various constitutive laws from the measurement of displacement, strains and/or prescribed forces. The most used methods are described in the useful review work of Avril et al. (2008). The selection of a suitable identification method is dependent on the constitutive model considered and on the experimental technique utilized to characterize the material behavior. A brief review of the main identification strategies, their compatibility with different constitutive behavior and with various experimental characterization procedures is developed in the next section. This is further utilized to select a suitable identification strategy according to the set of experimental data and the constitutive model selected. Section 3 briefly reviews the thermomechanical constitutive model selected (Chemisky et al., 2011) and presents the analytical expression of the macroscopic stress/strain state as a function of the internal variables and the model parameters. Section 4 presents the identification procedure based on the inverse procedure, with the definition of the analytical sensitivity matrix. The experimental validation for different thermomechanical loadings of the proposed method is presented in Section 4. Concluding remarks are provided in Section 5.

2. Selection of the parameter identification strategy for superelastic shape memory alloys

The requirements for the identification procedure adapted to the case of superelastic SMAs are the following:

i) The identification procedure should be adapted to the standard experimental tests utilized to characterize a superelastic SMA, i.e. proportional isothermal mechanical tests; ii) The procedure should be fast enough to be of a practical interest for the analysis of homogeneous standard superelastic tests; iii) This procedure should however be easily extended to the identification of model parameters based on more complex, heterogeneous tests assuming that full kinematic field are measured at the surface of the experiment using a suitable experimental technique. According to the last statement, the identification procedure should be based on those developed when full kinematic fields are experimentally measured. Five methods have been listed in the review of Avril et al. (2008). i.e: i) The constitutive equation gap method (CEGM); ii) the virtual fields method (VFM); iii) the equilibrium gap method (EGM) iv) the reciprocity gap method (RGM) and v) the finite element model updating method (FEMU).

The constitutive equation gap consists in the measurement of the distance between a given stress field and the corresponding stress field computed through the constitutive model from a given displacement field. This method has been recently extended to elastic–plastic behaviors (Latourte et al., 2008) or elastodynamics (Banerjee et al., 2013). Moussawi et al. (2013) have revisited the concept of constitutive relation error by introducing a constitutive compatibility of stress, which defines a subspace of the classical statically admissible stress space. The virtual fields method is based on the construction of virtual fields to extract material parameters (Avril and Pierron, 2007). This technique relies on the processing of the experimental strain fields when expressing the global equilibrium of a specimen through the principle of virtual work formulated with specific virtual displacement fields. It has been successfully applied to determine the elastic and damaged anisotropic behavior of composite materials (Chalal et al., 2004, 2006). This method requires a minimization of a cost function at each loading step to find the optimal parameters characteristic of a nonlinear behavior as reported in Grédiac and Pierron (2006). The equilibrium gap method and the reciprocity gap method have been developed, to the knowledge of the authors, only in the case of linear elasticity and are thus not adapted for the identification of material parameters for SMAs.

The finite element model updating method (FEMU) (Kavanagh and Clough, 1971), a very intuitive approach, is widely utilized for the model parameters identification. This method is nowadays widely used since it can be applied to non-linear constitutive laws and a wide variety of homogeneous and heterogeneous mechanical tests (Chaparro et al., 2008; Pottier et al., 2011).

The method proposed here is first specifically developed for homogeneous superelastic tests. A cost function can be written in terms of a least square difference between the experimental and the numerically evaluated components of the mechanical field. The minimization of the cost function can be achieved using deterministic algorithms such as gradient-based Levenberg–Marquardt algorithm (Levenberg, 1944; Marquardt, 1963), real space evolutionary-inspired, genetic algorithms or Bayesian statistical approaches (Beck and Arnold, 1977). Hybrid methods are also developed, that combine several methods (e.g. genetic and gradient-based, Chaparro et al., 2008); Aguir et al. (2011) have proposed a hybrid identification strategy coupling finite elements, neural network computations and genetic algorithm.

The Levenberg–Marquardt optimization algorithm has been often adopted for the determination of material parameters for metals (Springmann and Kuna, 2005; Mahnken and Stein, 1996; Ghouati and Gelin, 1998; Cooreman et al., 2007). Moreover, it has been shown that for the identification of elastic–plastic parameters the Levenberg–Marquardt algorithm is efficient in terms of accuracy, stability and computational cost compared to other optimization algorithms, i.e. evolutionary and hybrid algorithms (de-Carvalho et al., 2011; Chaparro et al., 2008). More recently, this algorithm has been extensively used for the constitutive law parameter identification of several types of material such as biopolymer composites (Brahim et al., 2013). Spranghers et al. (2014) proposed a damped least-squares solution based on the

Levenberg–Marquardt formulation to identify the plastic behavior of aluminum plates subjected to sudden blast loads. Moaveni et al. (2013) developed a sensitivity-based finite-element model updating strategy to identify, detect, locate, and quantify damage based on the changes in effective modal parameters. This optimization algorithm is therefore selected in the present work for the identification of the material parameters of shape memory alloys.

This method requires the computation of a sensitivity matrix, which contains the derivatives of the output (for instance the strain) components with respect to the material parameters. A good choice for the estimation of this sensitivity matrix may lead to less iteration and hence will reduce the computation cost. The numerical derivative using finite differences is the most commonly used technique to determine the derivatives with respect to the material parameters. It involves computation of the output (strain) for small perturbations of each model parameter. This requires $(n+1)$ FE simulations for each minimization iteration, where (n) refers to the total number of parameters that have to be identified. Finite differences technique is therefore computationally expensive and could also be inaccurate, leading to slower convergence or even divergence of the optimization procedure. Analytical method for matrix sensitivity computation has been proposed by Gavrus et al. (1996) using a differentiation of the discretized equilibrium equations. In this case, the sensitivity matrix is explicitly formulated through the analytical derivatives of the state variables (strains) with respect to the different model parameters. It requires, from the constitutive equations, a closed-form of the total strain as a function of the model parameters. Its main advantage consists in a closed-form sensitivity matrix leading to a substantial reduction of the computational cost, compared to the finite differentiation. Lecompte et al. (2007) applied this analytical estimation of the sensitivity matrix for the identification of the four in-plane orthotropic elastic constants of composite plate materials. Mahnken and Stein (1996) and Cooreman et al. (2007) applied such procedure in the case of viscoplastic and elastic–plastic constitutive models, respectively. Some authors proposed other determination schemes such as the mixed technique based on the semi-analytical method using the finite differentiation and analytical derivatives (Massoni et al., 2002; Barthelemy and Haftka, 1990), or adjoint methods (Bonnet, 1999; Tortorelli and Michaleris, 1994).

The description of the analytical sensitivity of each parameter on the material behavior thus requires that a set of analytical equations can be written between all the different state variables (i.e. the Cauchy stress/total strain, the absolute temperature and the set of internal variables). However, most of the constitutive models for SMAs proposed in the literature is formulated in terms of a system of partial differential equations (PDE) to be solved incrementally. It is therefore important to reduce such models to a system of standard constitutive equations which describe the material behavior for a proportional loading.

Among the models that can be found in the literature, the constitutive model developed by Chemisky et al. (2011) is selected, for the following reasons: i) the constitutive equations can be expressed as a closed-form function of model parameters in specific cases such as superelastic behavior under proportional loading; ii) the model considers several mechanisms, i.e. phase transformation, reorientation of martensitic variants and accommodation of twins in martensite. This will allow to extend the present work, that is focused on the superelastic behavior of SMAs, to other behavior such as reorientation; iii) the model is derived from a thermodynamic potential, which has an interest since the material parameters are related to physical features of the phase transformation (difference in specific internal energy, entropy, characteristic temperatures…). This allows hence to apply the present work for the identification model parameters of other thermodynamically based constitutive models for SMAs.

Motivated by the discussion presented in this section, the proposed work focuses on the development of an identification procedure for the parameters of the model of Chemisky et al. (2011), considering the assumption that the strain developed during the proportional loading path remains sufficiently small so that infinitesimal strain remains an acceptable measure of the deformation of the body.

3. Constitutive model for superelastic shape memory alloys

The Roundrobin performed by an international team where different constitutive models for shape memory were analyzed and their capability to describe several thermomechanical loading paths were compared (Sittner et al., 2009). Among the constitutive models developed to describe the thermomechanical behavior of shape memory alloys compared in this roundrobin, it has been shown that the model of Chemisky et al. (2011) is able to accurately describe the behavior of superelastic shape memory alloys. This model, briefly recalled here using the same notations, describes the behavior of a representative volume element (RVE), where four strain mechanisms contribute to the macroscopic strain response when a thermomechanical loading is applied i) the elastic strain ($\boldsymbol{\varepsilon}^e$), ii) the strain induced by the thermal expansion ($\boldsymbol{\varepsilon}^{th}$), iii) the transformation strain ($\boldsymbol{\varepsilon}^T$) and iv) the strain related to the accommodation of twins ($\boldsymbol{\varepsilon}^{twin}$). The transformation strain has been expressed as a function of the volume fraction of martensite f and the average transformation strain in the martensitic phase $\bar{\boldsymbol{\varepsilon}}^T$, such that $\boldsymbol{\varepsilon}^T = f\bar{\boldsymbol{\varepsilon}}^T$. In a similar fashion, the strain related to the accommodation of twins has been expressed as a function of the volume fraction of martensite created in a self-accommodated way f^{FA} and as the average transformation strain related to the accommodation of twins $\bar{\boldsymbol{\varepsilon}}^{twin}:\boldsymbol{\varepsilon}^{twin} = f^{FA}\cdot\bar{\boldsymbol{\varepsilon}}^{twin}$. This model is based on the thermodynamics of irreversible process to obtain the evolution equations of the internal variables that describe the state of the RVE. For more details and explanations regarding this model, the reader can refer to Chemisky et al. (2011). In what follows, an analytical formulation of the model is derived for the specific case of superelasticity as a function of the total strain, the model parameters, the stress and the temperature.

3.1. Analytical formulation of the constitutive model for phase transformation

It has been shown by Calloch et al. (2006) that during a proportional superelastic loading path, a linear relationship is established between the volume fraction of martensite and the transformation strain. Following Eq. (2.2) in Chemisky et al., 2011, this indicates that $\bar{\boldsymbol{\varepsilon}}^T$ remains constant during such loading paths. It is further considered, since during superelastic loadings the transformation occurs at a high stress level (typically hundreds of MPa), that the martensite appears in a fully oriented state. This has the following consequence on the value of the average transformation strain:

$$\left|\bar{\boldsymbol{\varepsilon}}^T\right| = \varepsilon^T_{SAT}. \tag{1}$$

This situation occurs when the critical stress magnitude to trigger the forward transformation σ^{Ms} is higher than the critical stress magnitude σ^f which corresponds to the end of the orientation mechanism. This situation is encountered during superelastic paths for common SMAs (NiTi, NiTiX and Cu-based alloys). These two considerations are valid when the following condition is verified:

During the evolution of the volume fraction of martensite, the other internal variables (i.e. $\bar{\varepsilon}^T$, $\bar{\varepsilon}^{twin}$, f^{FA}) remain constant during the complete thermomechanical loading path that starts from $T > A_f$, where (A_f) is the temperature of the end of reverse transformation from martensite to austenite.

A wide range of loading paths follow this assumption, and it is particularly valid for all proportional superelastic loading paths (e.g. isobaric tests under sufficiently high stress level). According to the evolution equation (2.28) of Chemisky et al. (2011) related to f^{FA}, if this internal variable does not evolve (the initial value of f^{FA} is zero) while the volume fraction of martensite evolves, it necessary means that $|\bar{\varepsilon}^T| = \varepsilon^T_{SAT}$ and $\boldsymbol{\varepsilon}^{twin}$=0, due to the formation of fully-oriented martensite only. The mean transformation strain can thus be written in the following form:

$$\bar{\varepsilon}^T_{ij} = \frac{3}{2}\varepsilon^T_{SAT}\eta_{ij}. \tag{2}$$

η_{ij} refers to the components of a direction tensor $\boldsymbol{\eta}$. The direction of the transformation force follows the orientation force (Chemisky et al., 2011), and in the case of proportional loading, the components of the direction tensor are proportional to the components of the deviatoric part of the stress tensor:

$$\eta_{ij} = \frac{\sigma'_{ij}}{|\boldsymbol{\sigma}|}. \tag{3}$$

Under the condition described in this section, Equations (2.28), (2.30) and (2.41) of Chemisky et al. (2011) allows to determine a closed-form expression for the evolution of the martensite volume fraction during the forward transformation:

$$f = \frac{1}{H_f}\left[\sigma_{ij}\bar{\varepsilon}^T_{ij} - \frac{1}{2}H_\varepsilon\bar{\varepsilon}^T_{ij}\bar{\varepsilon}^T_{ij} - B(T-T_0) - F_f^{crit}\right], F_f - F_f^{crit} = 0, \dot{f} > 0, \tag{4}$$

where H_f, H_ε are the hardening parameters for transformation and orientation, respectively. B is the entropy difference between martensite and austenite ($B = \Delta S = S^A - S^M$). T_0 is the equilibrium temperature and F_f and F_f^{crit} are the transformation force and the critical transformation force, respectively.

The critical force is written:

$$F_f^{crit} = F_f^{max} + \left(B_f - B\right)\cdot(T-T_0) - H_s\left|\bar{\varepsilon}^T\right|. \tag{5}$$

The term $(B_f - B)\cdot(T-T_0)$ arises from the difference of the hysteresis observed for a full thermomechanical cycle in the vicinity of the equilibrium temperature T_0. H_s is a term characteristic of the martensite stabilization mechanism. Combining relations (2), (4) and (5), and considering that the constraints $F_f - F_f^{crit} = 0, \dot{f} > 0$ are satisfied, the volume fraction of martensite yields:

$$f = \frac{1}{H_f}\left[|\sigma|\varepsilon^T_{SAT} - \frac{1}{2}H_\varepsilon\varepsilon^T_{SAT}\varepsilon^T_{SAT} - B_f(T-T_0) + H_s\varepsilon^T_{SAT} - F_f^{max}\right], \tag{6}$$

where $|\sigma|$ refers to the Mises equivalent stress. Note that this scalar closed-form equation is valid for any proportional loading. For the reverse transformation, during unloading and under same assumptions, the volume fraction of martensite can be written as:

$$f = \frac{1}{H_f}\left[|\sigma|\bar{\varepsilon}^T_{SAT} - \frac{1}{2}H_\varepsilon\varepsilon^T_{SAT}\varepsilon^T_{SAT} - B_r(T-T_0) + H_s\varepsilon^T_{SAT} + F_f^{max}\right]. \tag{7}$$

Considering that there is no thermal expansion during isothermal loading, and introducing two functions ϕ_1 *and* ϕ_2 defined as follows:

$$\phi_1 = 1 \text{ if } F_f = F_f^{crit}, 0 < f < 1 \;;\; \phi_1 = 0 \quad \text{otherwise}$$
$$\phi_2 = 1 \text{ if } f = 1; \phi_2 = 0 \quad \text{otherwise},$$

the following closed-form expression is therefore defined during a proportional loading in the case of isotropic elasticity:

$$\varepsilon^{tot}_{ij} = \frac{1}{E}\left[(1+\nu)\sigma_{ij} - \nu\sigma_{kk}\delta_{ij}\right] + \frac{3\varepsilon^T_{SAT}\eta_{ij}}{2H_f}\left[|\sigma|\varepsilon^T_{SAT} - \frac{1}{2}H_\varepsilon\varepsilon^T_{SAT}\varepsilon^T_{SAT} - B_f(T-T_0) + H_s\varepsilon^T_{SAT} - F_f^{max}\right]\phi_1 + \frac{3\varepsilon^T_{SAT}\eta_{ij}}{2H_f}\phi_2. \tag{8}$$

Note that the assumption of elastic isotropy is supported by the fact that most SMA polycrystals are not strongly textured and the fact that the amount of elastic strain remains small compared to the amount of transformation strain. The effect of elastic anisotropy, if any, will not induce a significant change in the total strain. Equation (8) corresponds to the closed-form expression of the total strain as a function of the state variables and the model parameters. A similar closed-form expression is found during a proportional unloading:

$$\varepsilon^{tot}_{ij} = \frac{1}{E}\left[(1+\nu)\sigma_{ij} - \nu\sigma_{kk}\delta_{ij}\right] + \frac{3\varepsilon^T_{SAT}\eta_{ij}}{2H_f}\left[|\sigma|\varepsilon^T_{SAT} - \frac{1}{2}H_\varepsilon\varepsilon^T_{SAT}\varepsilon^T_{SAT} - B_r(T-T_0) + H_s\varepsilon^T_{SAT} + F_f^{max}\right]\phi_1 + \frac{3\varepsilon^T_{SAT}\eta_{ij}}{2H_f}\phi_2. \tag{9}$$

A variable λ characteristic of the loading history is defined:

$\lambda = 1$ during the proportional loading;
$\lambda = 0$ during the proportional unloading

A unique expression for the total strain can thus be expressed:

$$\varepsilon^{tot}_{ij} = \frac{1}{E}\left[(1+\nu)\sigma_{ij} - \nu\sigma_{kk}\delta_{ij}\right] + \frac{3\varepsilon^T_{SAT}\eta_{ij}}{2H_f}\left[|\sigma|\varepsilon^T_{SAT} - \frac{1}{2}H_\varepsilon\varepsilon^T_{SAT}\varepsilon^T_{SAT} - B_f(T-T_0) + H_s\varepsilon^T_{SAT} - F_f^{max}\right]\phi_1\lambda + \frac{3\varepsilon^T_{SAT}\eta_{ij}}{2H_f}\left[|\sigma|\varepsilon^T_{SAT} - \frac{1}{2}H_\varepsilon\varepsilon^T_{SAT}\varepsilon^T_{SAT} - B_r(T-T_0) + H_s\varepsilon^T_{SAT} + F_f^{max}\right]\phi_1(1-\lambda) + \frac{3\varepsilon^T_{SAT}\eta_{ij}}{2H_f}\phi_2. \tag{10}$$

3.2. Physical interpretation of the model parameters – application to uniaxial superelastic loadings

Under the condition described in the previous section, it is possible to provide a physical interpretation of the model parameters that are characteristic of the phase transformation. For a uniaxial tension, Equation (7) reduces to

$$f = \frac{1}{H_f}\left[\sigma\varepsilon^T_{SAT} - \frac{1}{2}H_\varepsilon\varepsilon^T_{SAT}\varepsilon^T_{SAT} - B_f(T-T_0) + H_s\varepsilon^T_{SAT} - F_f^{max}\right] \tag{11}$$

The temperature M_s that corresponds to the onset of forward transformation is defined according to Eq. (11) when the stress level, the volume fraction of martensite and the mean transformation strain are zero. A relationship between M_s and F_f^{max} is thus established:

$$F_f^{max} = B_f(T_0 - M_s). \tag{12}$$

Writing Eq. (11) in the case of the onset of forward transformation (i.e. $f = 0$) leads to a condition for the onset of transformation temperature at zero stress and when the mean transformation strain magnitude reaches the saturation value:

$$T = M_s^* = \frac{1}{b_f}\left[-\frac{1}{2}H_\varepsilon \varepsilon_{SAT}^T + b_f M_s + H_s\right], \tag{13}$$

with $b_f \varepsilon_{SAT}^T = B_f$.

Note that this temperature corresponds to the intersection between the slope in the uniaxial stress–temperature phase diagram and the zero stress line. Practically, the identification of the two temperatures M_s and M_s^* should be determined from a zero-stress using DSC analysis and by the identification of the critical stress for the onset of forward transformation. This determination has to be performed at various temperatures to obtain the transformation limit slope at high stress. In the case of superelastic SMA, the identification procedure will be performed for isothermal proportional loading paths above A_f. In such a case, the DSC (Digital Scanning Calorimetry) analysis should be avoided because it is often difficult to estimate the transformation temperatures. Moreover, the transformation limits in the uniaxial stress–temperature diagram should be accurate in the range of stress that corresponds to superelastic loadings. It has been observed that these transformation limits are not linear for NiTi alloys (Wu et al., 2003), as shown in Fig. 1. It is clear that the transformation limits in the uniaxial stress–temperature diagram are not linear in the range of low stress levels while they are linear for high stress level. In Fig. 1, it is worth noticing that M_s^* does not coincide with M_s, which is the transformation temperature observed at zero stress. This difference is taken into account in the model of Chemisky et al. (2011) using the stabilization of martensite characteristic parameter, H_s. However, if the description of the transformation limits at low stress levels is not required, which is the case for superelastic loadings, the transformation temperatures M_s and M_s^* can be assumed to be identical, and the transformation limits in the phase diagram are considered as a slope for all stress levels. Thus, a relationship is introduced between H_ε and H_s:

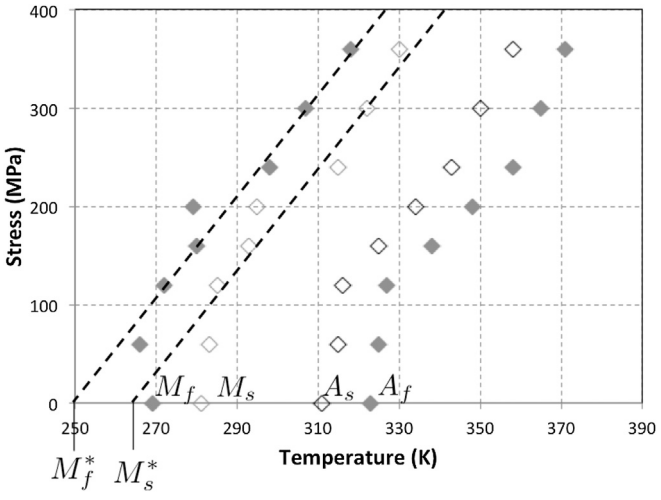

Fig. 1. Uniaxial stress–temperature diagram (from the isobaric experiments of Wu et al., 2003) that illustrates the difference of M_s and M_s^*.

Table 1
Physical interpretation of the model parameters to be identified for the superelastic behavior of SMAs.

Elastic	
E	Young modulus
ν	Poisson ratio
Transformation	
b_f	Slope in the uniaxial stress–temperature diagram for forward transformation
b_r	Slope in the uniaxial stress–temperature diagram for reverse transformation
ε_{SAT}^T	Transformation strain magnitude in the direction of the transformation
M_s	Temperature for the onset of forward transformation at zero stress
A_f	Temperature for the end of reverse transformation at zero stress
H_f	Transformation hardening parameter

$$H_s = \frac{1}{2}H_\varepsilon \varepsilon_{SAT}^T. \tag{14}$$

The volume fraction of martensite is therefore written:

$$f = \frac{\varepsilon_{SAT}^T}{H_f}\left[\sigma - b_f(T - M_s)\right]. \tag{15}$$

Under the same condition ($M_s = M_s^*$), and considering a uniaxial unloading path after a complete transformation, a similar relationship between the volume fraction of martensite as a function of the applied stress, the characteristic transformation temperature and the slope in the uniaxial stress–temperature phase diagram can be obtained. The temperature A_f that corresponds to the end of reverse transformation is defined according to Eq. (7) when the stress level, the volume fraction of martensite and the mean transformation strain are zero. The term F_f^{max} can thus be expressed as:

$$F_f^{max} = B_r\left(A_f - T_0\right). \tag{16}$$

With respect to the condition ($M_s = M_s^*$), the volume fraction of martensite in the case of uniaxial unloading is written as:

$$f = \frac{\varepsilon_{SAT}^T}{H_f}\left[\sigma - b_r\left(T - A_f\right)\right], \tag{17}$$

with $\varepsilon_{SAT}^T b_r = B_r$. Considering the case of superelastic proportional loadings, Table 1 summarizes the set of eight parameters that have to be identified.

4. Identification procedure

Having the set of model parameters defined in the last section, the next step is to develop an identification procedure aimed at extracting them simultaneously from experimental data. The identification problem considered here consists of retrieving the material parameters that minimize the difference between experimental and computed data using the reduced constitutive model presented in the previous section. The measurement of strain is chosen since different measurement techniques can be utilized in the case of superelastic proportional tests to obtain such experimental data. For example, strain gages, uniaxial or bi-axial extensometer can provide, from the information of elongation

over the measurement gage, average components of the strain tensor in this area. Also, optical techniques such as the Digital Image Correlation (DIC) can provide the displacement fields in the observed area from which the spatial distribution of longitudinal, transverse, and shear strains can be computed. For uniaxial homogeneous tests, the stress field is easily obtained from the prescribed forces and longitudinal and transverse strains are measured using a biaxial extensometer. The use of finite element analysis software is not required since the strain components can be derived directly from the proposed closed form (Eq. (10)) of the constitutive model. It is shown along this section that two isothermal loading paths are sufficient to retrieve the set of model parameters that describe the thermomechanical behavior of SMAs. Based on these considerations, the optimization problem can be expressed with the minimization of the following cost function (Meraghni et al., 2011):

$$C(p) = \frac{1}{2}\left(\boldsymbol{\varepsilon}(\boldsymbol{p})^{num} - \boldsymbol{\varepsilon}^{exp}\right)^T \boldsymbol{W}\left(\boldsymbol{\varepsilon}(\boldsymbol{p})^{num} - \boldsymbol{\varepsilon}^{exp}\right), \tag{18}$$

where $\boldsymbol{\varepsilon}(\boldsymbol{p})^{num}$ and $\boldsymbol{\varepsilon}^{exp}$ are two vectors that store the values of the three in-plane components of the strain for a number of time increments throughout a homogeneous loading path, considering multiple loading paths at different temperatures. $\boldsymbol{p}$ denotes the set of k guessed parameters, and $\boldsymbol{W}$ is the weighting matrix, and its diagonal components are $\|\boldsymbol{\varepsilon}_{\boldsymbol{xx}}^{exp}\|^{-2}$,$\|\boldsymbol{\varepsilon}_{\boldsymbol{yy}}^{exp}\|^{-2}$ or even $\|\boldsymbol{\varepsilon}_{\boldsymbol{xy}}^{exp}\|^{-2}$.

4.1. Description of the optimization algorithm

The minimization of the cost function can be solved through a gradient-based algorithm. The partial derivative of the cost function with respect to the material parameters is expressed as:

$$\frac{\partial C(p)}{\partial \boldsymbol{p}} = \left(\boldsymbol{\varepsilon}(\boldsymbol{p})^{num} - \boldsymbol{\varepsilon}^{exp}\right)^T \boldsymbol{W}\left(\frac{\partial \boldsymbol{\varepsilon}(\boldsymbol{p})^{num}}{\partial \boldsymbol{p}}\right). \tag{19}$$

In the right hand side of Equation (19), the first term corresponds to a vector where each component represents the difference between the numerically evaluated component of strain and its corresponding experimental value in terms of time, position and temperature. The third term is the Jacobian matrix that represents the local sensitivity of the strain components vector $\boldsymbol{\varepsilon}^{num}$ to variation in the components of the parameters vector $\boldsymbol{p}$. To find a set of parameters $\boldsymbol{p}$ that minimizes the cost function herein mentioned, the Levenberg–Marquardt (LM) algorithm is adopted, which has a guarantee of convergence (Fletcher, 1987) and is generally faster than a steepest descent algorithm. Therefore, this algorithm is unconditionally stable, and a local minimum is always obtained. This method does not however guarantee that a global minimum is found. A study of the influence of initial conditions is then necessary to check the numerical stability of the algorithm. The vectors of parameters at the increment $i+1$, $\boldsymbol{p}_{i+1}$, depends on the vectors of parameters at the increment i, $\boldsymbol{p}_i$ and a vector of updates $\Delta\boldsymbol{p}_i$:

$$\boldsymbol{p}_{i+1} = \boldsymbol{p}_i + \Delta\boldsymbol{p}_i \tag{20}$$

The vector of parameters updates $\Delta\boldsymbol{p}_i$ could be expressed through the following equation derived from the Levenberg–Marquardt algorithm computed at each iteration step i:

$$[\boldsymbol{S}_i^T\boldsymbol{W}\boldsymbol{S}_i + \boldsymbol{\mu}_i\,\mathrm{diag}(\boldsymbol{S}_i^T\boldsymbol{W}\boldsymbol{S}_i)]\Delta\boldsymbol{p}_i = \boldsymbol{S}_i^T\left(\boldsymbol{\varepsilon}(\boldsymbol{p}_i,t)^{num} - \boldsymbol{\varepsilon}(t)^{exp}\right). \tag{21}$$

If the regularization parameter $\boldsymbol{\mu}_i$ is zero, this algorithm reduces to the standard Gauss-Newton method. If μ takes a value sufficiently high, the effect of the component $\boldsymbol{S}_i^T\boldsymbol{W}\boldsymbol{S}_i$ becomes negligible and this algorithm reduces to a form of the gradient descent algorithm. The determination of the evolution of $\boldsymbol{\mu}_i$ is very important since the efficiency of the Levenberg–Marquardt algorithm mainly depends on this regularization parameter. The starting value of μ_1 is set to *100* for all the identification obtained in this paper. This means that the algorithm is close to a gradient descent algorithm at the beginning for a better stability. The following algorithm is applied at each increment i for the evolution of this parameter μ_i:

1 – Determine the set of parameters p_i^{μ}, $p_i^{10\mu}$, $p_i^{0.1\mu}$ with the current value of μ_i, $10\mu_i$ and $\mu_i/10$, respectively.

2 – Evaluate the cost function $C(p_i^{\mu})$, $C(p_i^{10\mu})$ and $C(p_i^{0.1\mu})$ with the three sets of parameters

3 – Apply the following condition:

IF $C(p_i^{\mu}) > C(p_{i-1})$ AND $C(p_i^{10\mu}) < C(p_{i-1})$ AND $C(p_i^{10\mu})$ is the minimum of $\{C(p_i^{\mu}), C(p_i^{10\mu}), C(p_i^{0.1\mu})\}$:

$\mu^{i+1} = 10\mu^i$

ELSE IF $C(p_i^{0.1\mu}) < C(p_{i-1})$ and $C(p_i^{0.1\mu})$ is the minimum of $\{C(p_i^{\mu}), C(p_i^{10\mu}), C(p_i^{0.1\mu})\}$:

$\mu^{i+1} = 0.1\mu^i$

ELSE

$\mu^{i+1} = \mu^i$

This method has privileged the reduction of μ when it seems to be more efficient and allows an increase of μ only when the cost function does not decrease any more with the current value of μ.

The derivation of the components of the sensitivity matrix using an analytical method is described below. In this work, a closed-form of the total strain has been expressed in the case of proportional loadings. It is therefore possible to obtain the analytical formulation of all the components of the Jacobian matrix **S**. According to Equation (10), a closed-form of the total strain is expressed. Each component of the strain tensor can be derived according to the following set of eight parameters:

$$\boldsymbol{p} := \left\{E, \nu, H_f, \varepsilon_{SAT}^T, b_f, b_r, M_s, A_f\right\} \tag{22}$$

The components of the first line of the analytical sensitivity matrix involving the strain component (ε_{11}^{num}) related to this set of parameters are:

$$S_{11} = \frac{\partial \varepsilon_{11}^{num}}{\partial E} = -\frac{1}{E^2}[(1+\nu)\sigma_{11} - \nu\sigma_{kk}], \tag{23}$$

$$S_{12} = \frac{\partial \varepsilon_{11}^{num}}{\partial \nu} = \frac{1}{E}[\sigma_{11} - \sigma_{kk}], \tag{24}$$

$$S_{13} = \frac{\partial \varepsilon_{11}^{num}}{\partial H_f} = -\frac{3\left(\varepsilon_{SAT}^T\right)^2 \eta_{11}}{2H_f^2}\left[\left[|\sigma| - \sigma_q^{M_s}\right]\phi_1\lambda + \left[|\sigma| - \sigma_q^{A_f}\right]\phi_1(1-\lambda)\right] - \frac{3\varepsilon_{SAT}^T \eta_{11}}{2H_f^2}\phi_2, \tag{25}$$

$$S_{14} = \frac{\partial \varepsilon_{11}^{num}}{\partial \varepsilon_{SAT}^T} = \frac{3\varepsilon_{SAT}^T \eta_{11}}{H_f}\left[\left[|\sigma| - \sigma_q^{M_s}\right]\phi_1\lambda + \left[|\sigma| - \sigma_q^{A_f}\right]\phi_1(1-\lambda)\right] + \frac{3\eta_{11}}{2H_f}\phi_2, \tag{26}$$

$$S_{15} = \frac{\partial \varepsilon_{11}^{num}}{\partial b_f} = -\frac{3\left(\varepsilon_{SAT}^T\right)^2 \eta_{11}}{2H_f}(T - M_s)\phi_1\lambda, \tag{27}$$

$$S_{16} = \frac{\partial \varepsilon_{11}^{num}}{\partial b_r} = -\frac{3\left(\varepsilon_{SAT}^T\right)^2 \eta_{11}}{2H_f}\left(T - A_f\right)\phi_1(1-\lambda), \tag{28}$$

$$S_{17} = \frac{\partial \varepsilon_{11}^{num}}{\partial M_s} = -\frac{3\left(\varepsilon_{SAT}^T\right)^2 \eta_{11}}{2H_f} b_f \phi_1 \lambda, \tag{29}$$

$$S_{18} = \frac{\partial \varepsilon_{11}^{num}}{\partial A_f} = -\frac{3\left(\varepsilon_{SAT}^T\right)^2 \eta_{11}}{2H_f} b_r (1-\lambda), \tag{30}$$

Note that all the derivatives of all the other components of $\boldsymbol{\varepsilon}^{num}$ are identical, except the derivatives with respect to E and ν, considering also the appropriate component of $\boldsymbol{\eta}$.

5. Identification of model parameters for NiTi SMAs: experimental validation of the proposed method

5.1. Material description and identification of the model parameters for a pseudo elastic NiTi SMA

The identification procedure is applied to determine the constitutive model parameters of a NiTi (50.6 at. % Ni), received in a fully annealed state and provided by Nimesis Technology. The material was annealed (673 K, 30 min) and water-quenched. Load controlled tensile tests have been conducted into a thermal chamber coupled to a uniaxial machine test having a capacity of 100 kN. Tensile tests were conducted at a crosshead speed of 2000 N/min. The tested specimens, dumbbell-shaped, were cut from thin plates (2.5 mm thickness) using waterjet hyperbaric machining. Their dimensions are given in Fig. 2. The strains in longitudinal (ε_{11}) and transverse (ε_{22}) directions have been measured by means of a biaxial extensometer positioned at the central zone of the specimen.

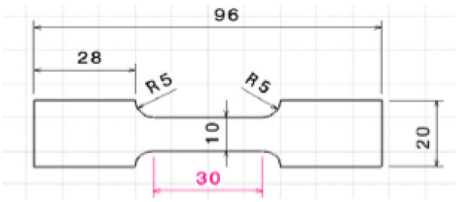

Fig. 2. Tensile specimen with 2.5 mm thickness.

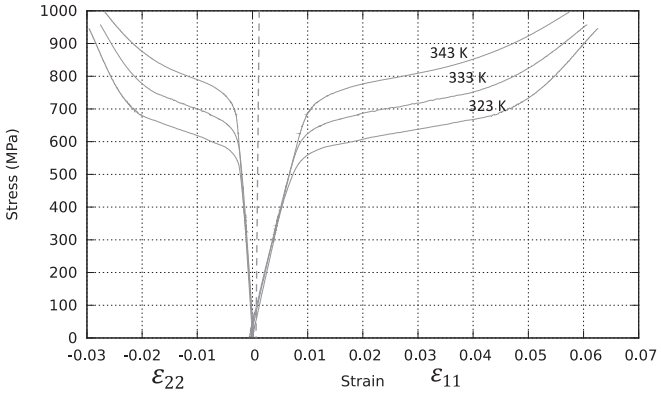

Fig. 3. Uniaxial stress–strain response of the NiTi superelastic alloy during three isothermal loadings.

The evolutions of the strain in the longitudinal and transverse directions according to the stress applied in the longitudinal direction are presented in Fig. 3. A single loading has been recorded, which is sufficient to determine the elastic parameters and the parameters characteristic of the forward transformation. Three tensile tests were performed at a temperature of 323 K, 333 K and 343 K, respectively. To identify all the material parameters from experimental results, a minimum of two tensile tests is required to obtain the stress–temperature dependence (represented in the model to be identified by the parameters b_f and b_r). In this following section, two tensile tests (at 323 K and 343 K) are utilized to identify the model parameters, and a third test performed at 333 K is exploited for the experimental validation of the identification procedure.

To validate the numerical stability of the identification procedure, several sets of initial parameters are used to obtain the final set of parameters. Numerical stability is thus considered to be

Table 2
Initial values for the five sets of parameters utilized for the validation of the identification procedure.

Set	E (MPa)	υ	H_f (MPa)	ε_{sat}^T	b_f (MPa/K)	b_r (MPa/K)	M_s (K)	A_f (K)
1	70 000	0.3	4	0.05	9.9	N/A	260	N/A
2	70 000	0.3	4	0.05	5	N/A	293	N/A
3	30 000	0.2	6	0.02	3	N/A	180	N/A
4	20 000	0.5	0.5	0.02	8	N/A	310	N/A
5	100 000	0.4	1	0.06	12	N/A	300	N/A

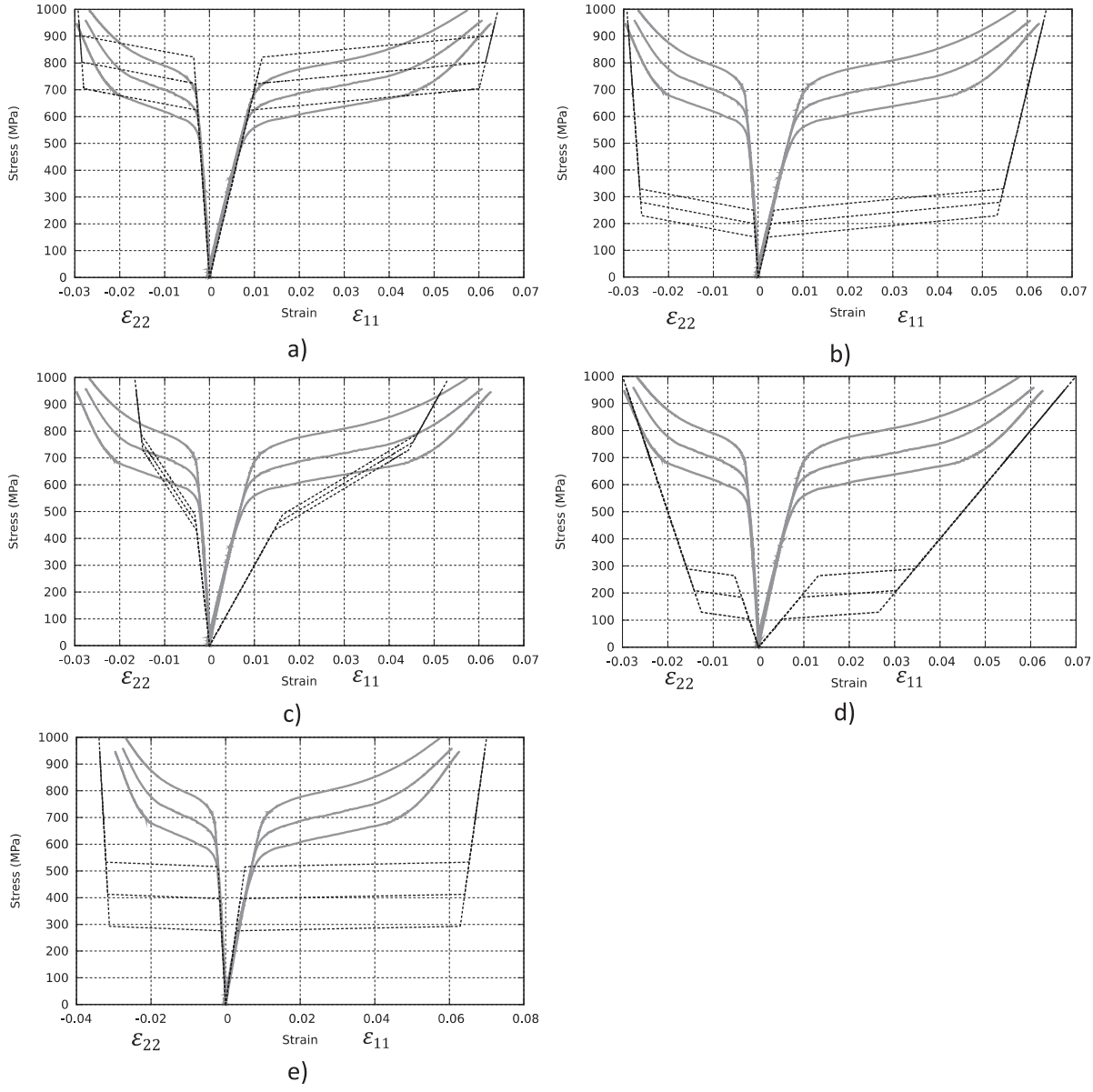

Fig. 4. Comparisons between the simulations (dashed black) of the uniaxial response using the initial set of parameters and the experimental response (plain gray) a) with the preliminary identification (PI) b) with the parameters provided in Chemisky et al. (2011). c), d) and e) with arbitrary initial sets of parameters. All these initial parameters are summarized in Table 2.

guaranteed if all these initial conditions lead to the same final (identified) set of parameters.

Table 2 presents the initial values of five sets of model parameters that are utilized for the identification procedure. The values of these parameters for the two first sets were chosen to correspond to those of Chemisky et al. (2011). In the first set, the values of b_f and M_s have been pre-identified based on an estimation of onset of the transformation using optimal values of the second derivative of the

Table 3
Identified values for the five sets of parameters, average identified values and coefficient of variation.

Set	E (MPa)	υ	H_f (MPa)	ε_{sat}^T	b_f (MPa/K)	b_r (MPa/K)	M_s (K)	A_f (K)
1	67 925.6	0.340122	8.18439	0.04269	9.41796	N/A	264.868	N/A
2	67 925.5	0.340122	8.18437	0.04269	9.41796	N/A	264.868	N/A
3	67 925.6	0.340122	8.18439	0.04269	9.41796	N/A	264.868	N/A
4	67 925.8	0.340121	8.18442	0.04269	9.41796	N/A	264.868	N/A
5	67 926.0	0.340120	8.18444	0.04269	9.41796	N/A	264.868	N/A
Average	67 925.7	0.340121	8.18440	0.04269	9.41796	N/A	264.868	N/A
Cov (%)	2.94E−04	2.63E−04	3.39E−04	0.00E+00	0.00E+00	N/A	0.00E+00	N/A

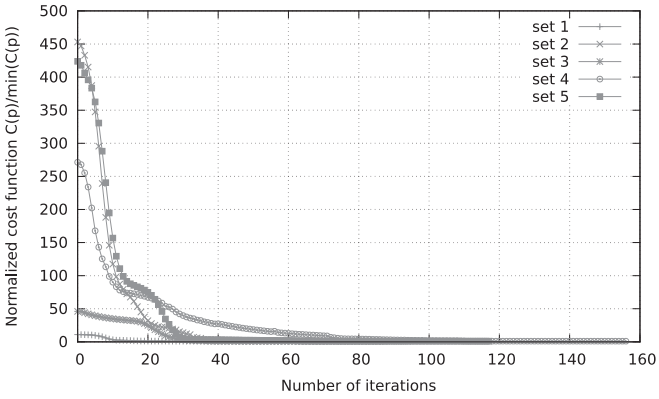

Fig. 5. Evolution of the cost function with the number of iterations for the five sets of initial parameters.

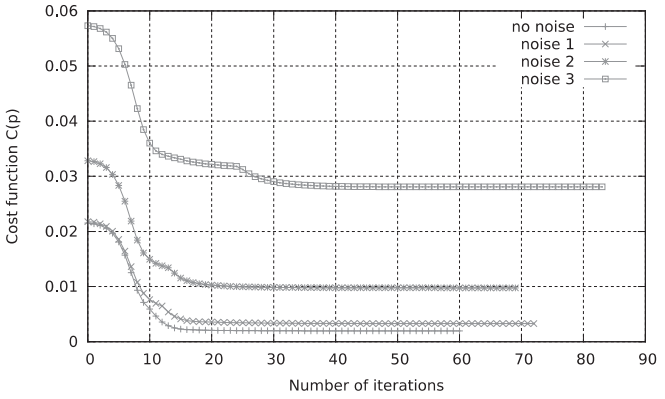

Fig. 7. Evolution of the cost function with the number of iterations for the four experimental data with various noise level.

strain with respect to the uniaxial stress. For the second set, the initial values were not modified. The values of the initial parameters of the three other sets have been chosen to represent a wide variety of behaviors, which are very different from the behavior of the studied SMA. The simulated responses of isothermal uniaxial tensile tests at the two temperatures utilized for the identification (323 K and 343 K), and at 333 K for the validation, are compared with the experimental response for these three temperatures (Fig. 4). The two parameters b_r and A_f, characteristic of the reverse phase transformation are not identified from these experimental data since only the forward transformation occurs.

Table 3 presents the values identified from the five sets of initial parameters. Note that all the final sets of parameters do not depend on the initial ones. Indeed, the Coefficient Of Variation over the five sets (COV in Table 3) is less than 10^{-3}% for all the parameters.

It is demonstrated that this method is robust and reliable, since the same set of identified parameters are found, regardless of the initial values. The number of iterations to reach a minimum of the cost function is compared for the five sets of initial parameters (see Fig. 5). It is clear that the pre-identification leads to a much faster convergence, since the value initial cost function is already low.

Combining the pre-identification and the identification procedure based on the analytical evaluation of the sensitivity matrix leads to a powerful tool for obtaining the model parameter of a SMA towards reliable simulations of the superelastic behavior of SMAs.

In Fig. 6, the simulated superelastic response is presented and compared to the three tension tests performed at 323 K, 333 K and 343 K, respectively. The simulated response over the SMA at 323 K and 343 K is compared to the experimental response utilized for the identification. In Fig. 7b the prediction of the superelastic behavior at 333 K computed on the basis of the parameters previously identified at 323 K and 343 K is compared to the experimental response at the same temperature. All the simulations (for the identification and the prediction) are very close to the experimental curves. It is thus confirmed that the identified parameters are reliable and can be utilized for the simulation of the superelastic response at various temperatures with a high accuracy (COV less than 1e-3%).

A sensitivity analysis of the influence of noise in the experimental data is performed next. The set of parameters identified with noisy data should correspond to the parameters identified previously to ensure the stability of the algorithm with respect to noise.

The stress-strain experimental data points were perturbed according to the following rule:

$$\begin{aligned} \tilde{\sigma}_{11} &= \sigma_{11} + \omega\ \delta_{\sigma} \\ \tilde{\varepsilon}_{11} &= \varepsilon_{11} + \omega\ \delta_{\varepsilon} \\ \tilde{\varepsilon}_{22} &= \varepsilon_{22} + \omega\ \delta_{\varepsilon} \end{aligned} \tag{31}$$

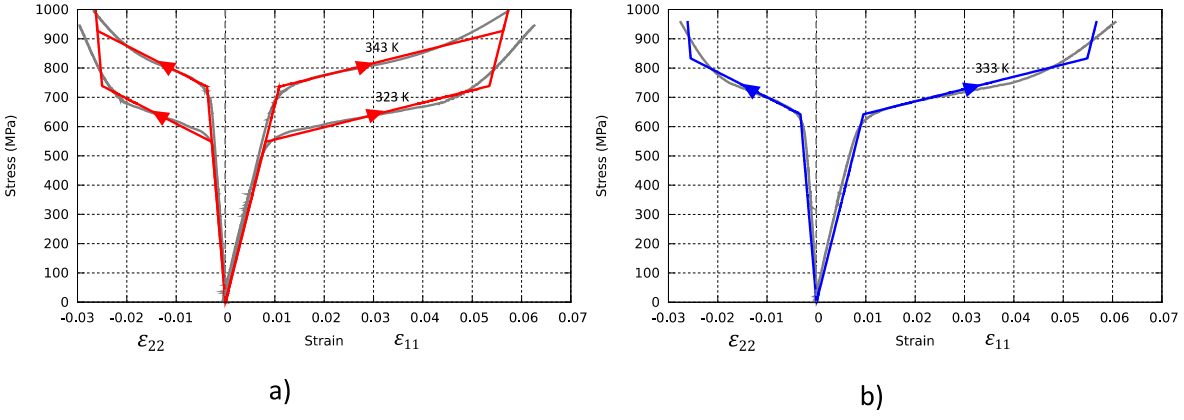

Fig. 6. Comparison between the simulated response and the experimental data a) for isothermal tests at the two temperatures utilized in the parameter identification procedure (323 K and 343 K). b) Experimental validation for an isothermal test at 333 K.

Table 4
Level of noise for the various sets of investigated experimental data.

Set	δ_σ (MPa)	δ_ε (%)
No noise	0	0
1	20	0.1
2	50	0.25
3	100	0.5

where ω is a random number in the range $[-1; 1]$ and δ_σ, δ_ε are scaling parameters. The sets of scaling parameters investigated are presented in Table 4

Table 5 shows the identified parameters for each of these sets. It is observed that the relative error increases while increasing the scaling parameter of noise, but in any case the relative error with respect to the parameters identified previously remains low (except for the hardening parameter H_f). This ensures that the identification procedure is stable and weakly sensitive to noise. The number of iterations to reach a minimum of the cost function is compared for the four sets of experimental data (see Fig. 7). It is observed that the number of iterations to reach convergence remains similar for each case. It can be concluded that the rate of convergence is not sensitive to noise.

A third study concerns the identification of the model parameters based on a combination of two or three experimental tests at different temperatures. The following sets of experiments are utilized for the identification:

- Set 1: Identification from the tests performed at 323 K, 333 K.
- Set 2: Identification from the tests performed at 323 K, 343 K (set utilized for the identification of the parameters found in Table 3).
- Set 3: Identification from the tests performed at 333 K, 343 K.
- Set 4: Identification from the tests performed at 323 K, 333 K, 343 K.

The initial guessed parameters correspond to the pre-identified set. Table 6 summarizes the identified parameters obtained in each case. It is noted that, since the coefficient of variation for every parameter is always less than 5%, the model predicts with a high accuracy the behavior of such alloy in this range of temperature since a single set of parameters is sufficient to describe the behavior of the material.

Note also that the proposed identification method that uses an analytical sensitivity matrix is very fast, since no numerical simulation has to be performed (by means of FEA or other numerical simulation tools). Therefore, it takes only a few seconds to identify the set of eight parameters even if the initial parameters have not been pre-identified. Running FEA analysis with a standard finite difference scheme for the computation of the sensitivity matrix is very time consuming since $1 + k$ numerical simulations are required at each increment (k being the number of parameters to identify).

5.1.1. Validation using experimental data from the literature (Lagoudas et al., 2012)

The proposed identification procedure has been utilized to obtain the model parameters corresponding to the behavior of the NiTi alloy tested in superelastic loadings. The identified model has shown that it is able to predict with a good agreement the behavior of this alloy.

In the following section, the identification procedure is applied to obtain the model parameters of a second superelastic behavior of a NiTi alloy exhibiting a reverse martensite transformation. This second application is aimed at demonstrating the capability of the proposed identification approach to extract the whole set of the eight model parameters including those characterizing the reverse transformation, namely: b_r and A_f.

The specimen, a NiTi wire (50.8 at %Ni, provided by Memry Corporation) of diameter 0.5 mm has been characterized by Lagoudas et al. (2012) at three temperatures by loading-unloading tensile test at a strain rate of 3.10^{-4}/s.

Three isothermal superelastic tests were performed at $T = 313$ K, $T = 303$ K and $T = 298$ K (see Fig. 8). It is noted in Lagoudas et al. (2012) that the stress-induced transformation into martensite is not fully completed by 700 MPa for any of the temperatures shown. It is also observed that the reverse transformation, which is complete since there is no residual at the end of a full cycle, is very smooth, especially at the end of the transformation. These features are not captured by using a linear transformation hardening law,

Table 5
Identified values for the four sets of experimental data with various noise level.

Set	E (MPa)	υ	H_f (MPa)	ε^T_{sat}	b_f (MPa/K)	b_r (MPa/K)	M_s (K)	A_f (K)
No noise	67 925.6	0.340122	8.18439	0.04269	9.41796	N/A	264.868	N/A
1	67 530.2	0.340053	8.27990	0.042757	9.42473	N/A	264.917	N/A
Error (%)	0.60	0.02	1.17	0.16	0.07	N/A	0.02	N/A
2	68 284.5	0.335907	9.23409	0.0430137	9.61292	N/A	267.463	N/A
Error (%)	0.53	1.24	12.8	0.76	2.07	N/A	0.98	N/A
3	68 181.7	0.342353	11.1228	0.0424649	9.65614	N/A	270.339	N/A
Error (%)	0.38	0.66	35.9	0.53	2.53	N/A	2.07	N/A

Table 6
Identified values for the four sets of experimental data, average identified values and coefficient of variation.

Set	E (MPa)	ν	H_f (MPa)	ε^T_{sat}	b_f (MPa/K)	b_r (MPa/K)	M_s (K)	A_f (K)
1	67 705.6	0.32593	7.85877	0.04316	8.79485	N/A	260.11	N/A
2	67 925.6	0.34012	8.18439	0.04269	9.41796	N/A	264.87	N/A
3	72 544.3	0.30945	8.49679	0.04229	9.93330	N/A	269.94	N/A
4	69 703.9	0.32457	8.33538	0.04298	9.40574	N/A	265.20	N/A
Average	69 469.8	0.32502	8.21883	0.04278	9.38796	N/A	265.03	N/A
Cov (%)	3.22	3.86	3.31	0.88	4.96	N/A	1.51	N/A

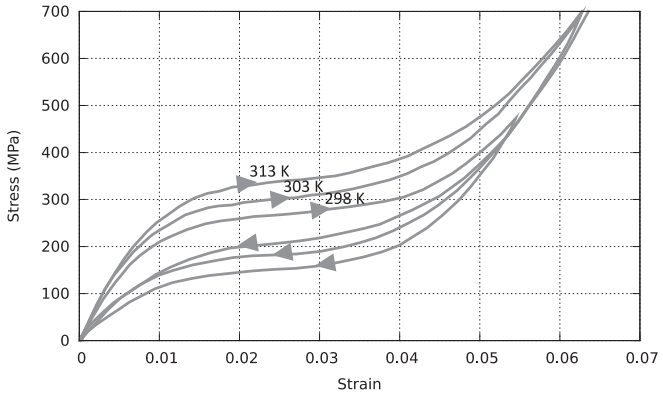

Fig. 8. Experimental isothermal uniaxial tensile tests at three temperatures: $T = 313$ K, $T = 303$ K and $T = 298$ K performed by Lagoudas et al. (2012).

Table 7
Initial set of parameters utilized for the identification procedure.

E (MPa)	ν	H_f (MPa)	ϵ_{sat}^T	b_f (MPa/K)	b_r (MPa/K)	M_s (K)	A_f (K)
70 000	0.3	4	0.05	4.9	3.8	244	258

Table 8
Identified set of parameters from uniaxial tests at 298 K and 313 K.

E (MPa)	ν	H_f (MPa)	ϵ_{sat}^T	b_f (MPa/K)	b_r (MPa/K)	M_s (K)	A_f (K)
24 500	0.3	3.3	0.032	5.42	4.0	257	273

and lead to the definition of an apparent modulus for the part which is assumed to be elastic. Indeed, the behavior is not purely elastic but presents a low apparent modulus (lower than what is expected for a near-equiatomic NiTi alloy).

In this characterization, no information for the evolution of strains in the other directions were recorded, thus the Poisson ratio cannot be extracted from these experimental data. It has been assumed to be 0.3, the same value assumed in Lagoudas et al. (2012). Initial parameters are taken to be the same as the set of parameters utilized in Chemisky et al. (2011), except the values b_f,b_r,M_s,A_f that have been pre-identified using the pre-identification procedure described in Section 3.2. This initial set of parameters is presented in Table 7.

The identified parameters are given in Table 8. Fig. 9a shows the simulation of the stress-strain curves based on this identification procedure at 298 K and 313 K. Fig. 9b shows the simulation of an isothermal tension test at 303 K, which has not been used for the identification of the model parameters. It is shown that the identification procedure is able to obtain the model parameters that correspond to the behavior of other SMAs tested in the literature.

6. Concluding remarks and further work

In this work, an identification procedure of the whole set of model parameters governing a superelastic shape memory alloy has been developed. An analytical form of the constitutive model of Chemisky et al. (2011) has been derived for isothermal proportional loadings. This form has led to the formulation of an analytical sensitivity matrix integrated into the gradient-based optimization algorithm (Levenberg–Marquardt). A cost function, based on the square gap between numerical (predicted) and experimental (measured) components of the longitudinal and transverse strain is minimized to find the optimal set of parameters. To improve the convergence rate, a pre-identification method, based on the second derivatives of the strain component with respect to their corresponding stress component has been implemented. This also allows to start with initial parameter that will trigger a phase transformation in the range of considered stress. This aspect constitutes a necessary condition for the identification of the model parameters related to the phase transformation.

The developed identification approach has been successfully applied for the identification of two superelastic SMAs. It is found that the developed method is robust and efficient for extracting model parameters from experimental data. Combining these two tools provides a reliable tool for the identification of the model parameters towards the simulation of the superelastic response of SMAs.

Further work will focus on the model parameter identification for biaxial tests where the strain fields are measured using Digital Image Correlation (DIC). Additional model parameters related to the characteristic of the orientation of martensite, the tension-compression asymmetry and to the internal (partial) loops will be included in the parameter identification process that will be extended for this purpose.

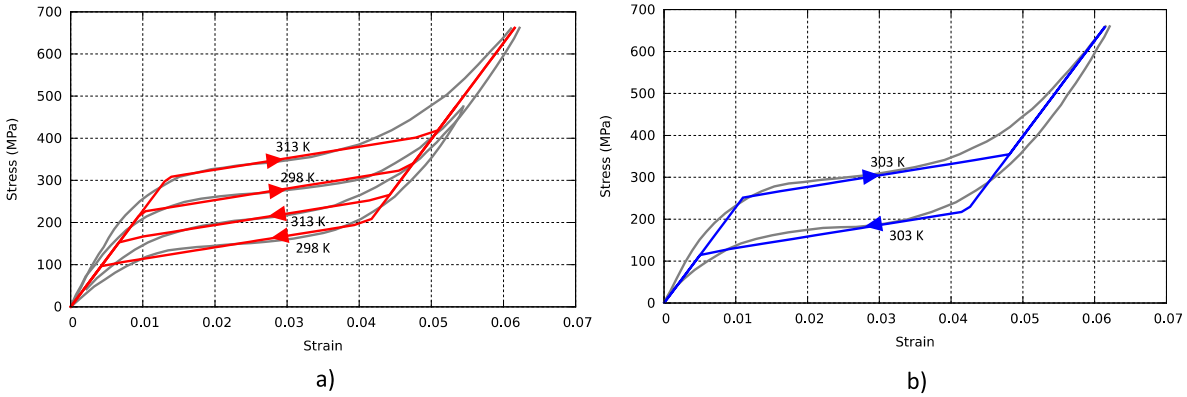

Fig. 9. Comparison between simulation using the identified model parameters and the experimental response in uniaxial tension a) For the two isothermal tests at the temperatures utilized for the identification (298 K, 313 K). b) at 303 K, temperature for the experimental validation.

References

Aguir, H., BelHadjSalah, H., Hambli, R., 2011. Parameter identification of an elasto-plastic behaviour using artificial neural networks–genetic algorithm method. Mater. Des. 32, 48–53.

ASTM Standard F2004, 2005–2010. Test Method for Transformation Temperature of Nickel-Titanium Alloys by Thermal Analysis.

ASTM Standard F2082, 2006. Test Method for Determination of Transformation Temperature of Nickel-Titanium Shape Memory Alloys by Bend and Free Recovery.

Avril, S., Pierron, F., 2007. General framework for the identification of constitutive parameters from full-field measurements in linear elasticity. Int. J. Solids Struct. 44, 4978–5002.

Avril, S., Bonnet, M., Bretelle, A., Grediac, M., Hild, F., Ienny, P., Latourte, F., Lemosse, D., Pagano, S., Pagnacco, E., Pierron, F., 2008. Overview of identification methods of mechanical parameters based on full-field measurements. Exp. Mech. 48, 381–402.

Banerjee, B., Walsh, T.F., Aquino, W., Bonnet, M., 2013. Large scale parameter estimation problems in frequency-domain elastodynamics using an error in constitutive equation functional. Comput. Methods Appl. Mech. Eng. 253, 60–72.

Barthelemy, B., Haftka, R.T., 1990. Accuracy analysis of the semi-analytical method for shape sensitivity analysis. Mech. Struct. Mach. 18, 407–432.

Beck, J.V., Arnold, K.J., 1977. Parameter Estimation in Engineering and Science. In: Wiley Series in Probability and Mathematical Statistics. J. Wiley, New York.

Bonnet, M., 1999. A general boundary-only formula for crack shape sensitivity of integral functionals. C. R. l'Acad. Sci. Ser. IIB Mech. Phys. Astron. 327, 1215–1221.

Brahim, E., Guessasma, S., Imad, A., Benseddiq, N., 2013. Identification of the mechanical behaviour of biopolymer composites using multistart optimisation technique. Mater. Des. 2013, 391–397.

Calloch, S., Taillard, K., Arbab Chirani, S., Lexcellent, C., Patoor, E., 2006. Relation between the martensite volume fraction and the equivalent transformation strain in shape memory alloys. Mater. Sci. Eng. A 438–440, 441–444.

Chalal, H., Meraghni, F., Pierron, F., Grédiac, M., 2004. Direct identification of the damage behaviour of composite materials using the virtual fields method. Compos. Part Appl. Sci. Manuf. 35, 841–848.

Chalal, H., Avril, S., Pierron, F., Meraghni, F., 2006. Experimental identification of a nonlinear model for composites using the grid technique coupled to the virtual fields method. Compos. Part A 37, 315–325.

Chaparro, B.M., Thuillier, S., Menezes, L.F., Manach, P.Y., Fernandes, J.V., 2008. Material parameters identification: gradient-based, genetic and hybrid optimization algorithms. Comput. Mater. Sci. 44, 339–346.

Chemisky, Y., Duval, A., Patoor, E., Ben Zineb, T., 2011. Constitutive model for shape memory alloys including phase transformation, martensitic reorientation and twins accommodation. Mech. Mater. 43 (7), 361–376.

Cooreman, S., Lecompte, D., Sol, H., Vantomme, J., Debruyne, D., 2007. Elasto-plastic material parameter identification by inverse methods: calculation of the sensitivity matrix. Int. J. Solids Struct. 44, 4329–4341.

de-Carvalho, R., Valente, R.A.F., Andrade-Campos, A., 2011. Optimization strategies for non-linear material parameters identification in metal forming problems. Comput. Struct. 89, 246–255.

Fletcher, R., 1987. Practical Methods of Optimization, second ed. John Wiley & Sons.

Gavrus, A., Massoni, E., Chenot, J.L., 1996. An inverse analysis using a finite element model for identification of rheological parameters. J. Mater. Process. Technol. 60, 447–454.

Ghouati, O., Gelin, J.C., 1998. Identification of material parameters directly from metal forming processes. J. Mater. Process. Technol. 80–81, 560–564.

Grédiac, M., Pierron, F., 2006. Applying the virtual fields method to the identification of elasto-plastic constitutive parameters. Int. J. Plasticity 22, 602–627.

Hartl, D., Lagoudas, D.C., Mabe, J., Calkins, F., 2010a. Use of Ni60Ti shape memory alloy for active jet engine chevron application, Part I: thermomechanical characterization. Smart Mater. Struct. 19 (1).

Hartl, D., Lagoudas, D.C., Mabe, J., Calkins, F., Mooney, J., 2010b. Use of Ni60Ti shape memory alloy for active jet engine chevron application, Part II: experimentally validated numerical analysis. Smart Mater. Struct. 19 (1).

Kavanagh, K., Clough, R., 1971. Finite element applications in the characterization of elastic solids. Int. J. Solids Struct. 7, 11–23.

Lagoudas, D.C. (Ed.), 2008. Shape Memory Alloys: Modeling and Engineering Applications. Springer.

Lagoudas, D.C., Entchev, P., Popov, P., Patoor, E., Brinson, L.C., Gao, X., 2006. Shape memory alloys – part II: modeling of polycrystals. Mech. Mater. 38, 430–462.

Lagoudas, D.C., Hartl, D.J., Chemisky, Y., Machado, L., Popov, L., 2012. Constitutive model for the numerical analysis of phase transformation in polycrystalline shape memory alloys. Int. J. Plasticity 32–33, 155–183.

Latourte, F., Chrysochoos, A., Pagano, S., Wattrisse, B., 2008. Elastoplastic behavior identification for heterogeneous loadings and materials. Exp. Mech. 48, 435–449.

Lecompte, D., Smits, A., Sol, H., Vantomme, J., Van Hemelrijck, D., 2007. Mixed numerical-experimental technique for orthotropic parameter identification using biaxial tensile tests on cruciform specimens. Int. J. Solids Struct., 1643–1656.

Levenberg, K., 1944. A method for the solution of certain non-linear problem in least squares. Q. Appl. Math. 2, 164–168.

Mahnken, R., Stein, E., 1996. Parameter identification for viscoplastic models based on analytical derivatives of a least-squares functional and stability investigations. Int. J. Plasticity 12, 451–479.

Marquardt, D.W., 1963. An algorithm for least-squares estimation of nonlinear parameters. J. Soc. Ind. Appl. Math. 11 (2), 431–441.

Massoni, E., Boyer, B., Forestier, R., 2002. Inverse analysis of thermomechanical upsetting tests using gradient method with semi-analytical derivatives. Int. J. Therm. Sci. 41, 557–563.

Meraghni, F., Nouri, H., Bourgeois, N., Czarnota, C., Lory, P., 2011. Parameters identification of fatigue damage model for short glass fiber reinforced polyamide (PA6-GF30) using digital image correlation. Proc. Eng. 10, 2110–2116.

Moaveni, B., Stavridis, A., Lombaert, G., Conte, J.P., Shing, P.B., 2013. Finite-element model updating for assessment of progressive damage in a 3-story infilled RC Frame. J. Struct. Eng. (U. S.) 139, 1665–1674.

Moussawi, A., Lubineau, G., Florentin, E., Blaysat, B., 2013. The constitutive compatibility method for identification of material parameters based on full-field measurements. Comput. Methods Appl. Mech. Eng. 265, 1–14.

Otsuka, K., Wayman, C.M., 1999. Shape Memory Materials. Cambridge University Press.

Patoor, E., Lagoudas, D.C., Entchev, P., Brinson, L.C., Gao, X., 2006. Shape memory alloys, part I: general properties and modeling of single crystals. Mech. Mater. 38 (5–6), 391–429.

Pottier, T., Toussaint, F., Vacher, P., 2011. Contribution of heterogeneous strain field measurements and boundary conditions modelling in inverse identification of material parameters. Eur. J. Mech. - A/Solids 30, 373–382.

Sittner, P., Heller, L., Pilch, J., Sedlak, P., Frost, M., Chemisky, Y., Duval, A., Piotrowski, B., Ben Zineb, T., Patoor, E., Auricchio, F., Morganti, S., Reali, A., Rio, G., Favier, D., Liu, Y., Gibeau, E., Lexcellent, C., Boubakar, L., Hartl, D., Oehler, S., Lagoudas, D.C., Van Humbeeck, J., 2009. Roundrobin SMA Modeling, ESOMAT 2009-8th European Symposium on Martensitic Transformations. EDP Sciences.

Spranghers, K., Vasilakos, I., Lecompte, D., Sol, H., Vantomme, J., 2014. Identification of the plastic behavior of aluminum plates under free air explosions using inverse methods and full-field measurements. Int. J. Solids Struct. 51, 210–226.

Springmann, M., Kuna, M., 2005. Identification of material parameters of the Gurson-Tvergaard-Needleman model by combined experimental and numerical techniques. Comput. Mater. Sci. 32, 544–552.

Stebner, A., Hartl, D., Chemisky, Y., Benefan, O., Turner, T., Calkins, F.T., Padula, S., Seelecke, S., Brinson, L.C., Lagoudas, D.C., 2011. Development of frameworks for comparing shape memory Alloy models: 3-D phenomenological continuum models. In: ASME 2011 Conference on Smart Materials, Adaptive Structures, & Intelligent Systems, Scottsdale, AZ, USA.

Tortorelli, D.A., Michaleris, P., 1994. Design sensitivity analysis: overview and review. Inverse Problems Eng. 1, 71–105.

Wu, X.D., Sun, G.J., Wu, J.S., 2003. The nonlinear relationship between transformation strain and applied stress for nitinol. Mater. Lett. 57, 1334–1338.